Clinical & Experimental Immunology
The Journal of Translational Immunology

Clinical and Experimental Immunology ORIGINAL ARTICLE doi:10.1111/cei.12668

IL-1R1 is expressed on both Helios$^+$ and Helios$^-$FoxP3$^+$CD4$^+$ T cells in the rheumatic joint

M. Müller, J. Herrath and V. Malmström
Rheumatology Unit, Department of Medicine, Karolinska University Hospital Solna, Karolinska Institutet, Stockholm, Sweden

Accepted for publication 12 June 2015
Correspondence: M. Müller, Rheumatology Research Unit, CMM L8:04, Karolinska University Hospital, 171 76 Stockholm, Sweden.
E-mail: malin.muller@ki.se

Summary

Synovial fluid from rheumatic joints displays a well-documented enrichment of forkhead box protein 3 (FoxP3)$^+$ regulatory T cells (tissue T_{regs}). However, we have previously demonstrated that the mere frequency of FoxP3 expressing cells cannot predict suppressive function. Instead, extrinsic factors and the functional heterogeneity of FoxP3$^+$ T_{regs} complicate the picture. Here, we investigated FoxP3$^+$ T_{regs} from blood and synovial fluid of patients with rheumatic disease in relation to Helios expression by assessing phenotypes, proliferative potential and cytokine production by flow cytometry. Our aim was to investigate the discriminatory potential of Helios when studying FoxP3$^+$ T_{regs} in an inflammatory setting. We demonstrate that the majority of the synovial FoxP3$^+$CD4$^+$ T cells in patients with inflammatory arthritis expressed Helios. Helios$^+$FoxP3$^+$ T_{regs} displayed a classical T_{reg} phenotype with regard to CD25 and cytotoxic T lymphocyte-associated antigen (CTLA)-4 expression and a demethylated T_{reg}-specific demethylated region (TSDR). Furthermore, Helios$^+$FoxP3$^+$ T cells were poor producers of the effector cytokines interferon (IFN)-γ and tumour necrosis factor (TNF), as well as of the anti-inflammatory cytokine interleukin (IL)-10. The less abundant Helios$^-$FoxP3$^+$ T cell subset was also enriched significantly in the joint, displayed a overlapping phenotype to the double-positive T_{reg} cells with regard to CTLA-4 expression, but differed by their ability to secrete IL-10, IFN-γ and TNF upon T cell receptor (TCR) cross-linking. We also demonstrate a striking enrichment of IL-1R1 expression in synovial CD4$^+$ T cells that was restricted to the CD25-expressing FoxP3 population, but independent of Helios. IL-1R1 expression appears to define a tissue T_{reg} cell phenotype together with the expression of CD25, glucocorticoid-induced TNF receptor family-related gene (GITR) and CTLA-4.

Keywords: FoxP3, Helios, inflammatory arthritis, Human regulatory T cells, tissue T_{reg} cells, IL1R1

Introduction

Regulatory T cells (T_{regs}) are central in immune homeostasis and in preventing autoimmune disease [1]. T_{reg} prevalence and functionality in different settings of autoimmune disease has been studied extensively, both for understanding whether T_{reg} deficiency is part of the disease aetiology and for setting a basis for T_{reg}-mediated therapeutic approaches [2].

Today, T cells with immune-modulating properties show a high degree of heterogeneity, even though the discovery of the T_{reg} lineage marker forkhead box protein 3 (FoxP3: forkhead–winged helix transcription factor) made a more precise characterization of different T_{reg} phenotypes possible [3,4]. FoxP3 is expressed in natural T_{regs} (nT_{regs}) and in T_{regs} induced in the periphery (iT_{regs}), the absence of a functional FoxP3 gene leads to severe immunopathology both in mice [5,7] and humans [6,8]. Cytotoxic T lymphocyte-associated antigen (CTLA)-4 is another essential molecule for T_{reg} function [9], where deficiency leads to immunopathology in mice [10,11] and humans [12].

Helios belongs to the Ikaros gene family of zinc-finger DNA-binding proteins, which have important roles during embryonic haematopoiesis and the development of immunity [13]. Helios is also expressed in haematopoietic stem cells (HSC), but thereafter is largely restricted to T cells. Helios was put forward initially as a marker that could distinguish between nT_{regs} and iT_{regs} [14,15]. However, evidence has emerged more recently also showing expression of Helios, in certain conditions, in iT_{regs}. Helios appears to be associated more with the path of activation rather than the origin of these cells [16,17]. However, it has been of interest to distinguish Helios$^+$ from Helios$^-$ T_{regs} as some functional differences have been suggested, such as the ability to produce cytokines [18,19]. Recently, surface expression of IL-1R1 (IL-1 receptor type 1) in conjunction with CCR7 has been shown to be a useful combination of cell surface markers to distinguish Helios$^-$ T_{regs} from Helios$^+$ T cells [20]. The IL-1R1 is expressed predominantly on T cells, fibroblasts and endothelial cells, where it conducts its biological inflammatory functions by binding IL-1α and IL-1β [21].

Inflammatory rheumatic diseases are complex chronic disorders where inflammation in synovial joints results in destruction of bone, cartilage and connective tissue. We, as well as others, have demonstrated previously that FoxP3$^+$ T_{regs} accumulate at the site of inflammation [22,23] and that the local milieu can affect T_{reg} functionality [24–26]. Such effects have also been demonstrated in other disease settings, such as type 1 diabetes and cancer [27–29]. An ongoing debate is whether the observed FoxP3$^+$ T_{reg} enrichment at inflammatory sites represent true T_{regs} or simply CD4$^+$ T cells transiently up-regulating FoxP3; hence, there is a continued need to further dissect T_{regs}, e.g. in the rheumatic joint. The relative accessibility of cells from inflamed joints, as patients may need joint effusions as part of their clinical care, makes arthritis a useful prototype model for studying sites of chronic inflammation.

In this study, we show that Helios$^+$ FoxP3$^+$ T_{regs} represent the major subpopulation of T_{regs} in the joint. Among the investigated parameters, two aspects segregated the Helios$^+$ from the Helios$^-$ FoxP3$^+$ T cell population, where the former subset expressed more CD25 and the latter displayed an ability to secrete cytokines. CTLA-4 expression in the joint was equally high on both subsets, and the epigenetic profile of the demethylated T_{reg}-specific demethylated region (TSDR) was also comparable, even though the Helios$^+$ FoxP3$^+$ T cells showed the least variation. While IL-1R1 and CCR7 co-expression could distinguish Helios$^-$ from Helios$^+$FoxP3$^+$ T cells in peripheral blood (PB), this combination of cell surface markers was not useful in synovial fluid (SF). Strikingly, IL-1R1 expression was highly up-regulated in SF but without association to Helios (or CCR7), and it was restricted to the CD25^{high}FoxP3$^+$ T_{reg} cell population.

Materials and methods

Patients

PB and SF samples were collected from the Rheumatology Clinic at time-points of active inflammation (relapses) in large joints requiring joint effusion, and mononuclear cells were prepared by Ficoll separation (Ficoll-Paque, Pharmacia, Sweden) and cryopreserved. A total of 46 patients were included in this study, 28 female and 18 male, with a median age of 55 years (min. 26, max. 85 years). Of these 46 patients, 22 were diagnosed with rheumatoid arthritis (RA), 17 with spondarthropathy (SpA), five with juvenile arthritis (JIA) and two with reactive arthritis. Healthy controls (HC) $n = 13$, nine female and four male, median age 35 years (23–50 years), were included into this study. For the phenotypical analysis of SF and PB, different numbers of patients were included for different markers, as follows: Helios FoxP3 subpopulations; $n = 33$ (17 SpA, five JIA, 10 RA and one reactive arthritis), CD25; $n = 33$ analysis (17 SpA, five JIA, 10 RA and one reactive arthritis), glucocorticoid-induced tumour necrosis factor (TNF)-related family-related gene (GITR); $n = 15$ (nine SpA and six RA), CTLA-4; $n = 17$ (12 SpA, one JIA, four RA) and for CD62L; $n = 27$ (17 SpA, five JIA, four RA and one reactive arthritis). For the same analysis in PB, the number of patients and spread of diagnosis were as follows; Helios FoxP3 subpopulations; $n = 35$ (14 SpA, 19 RA and two reactive arthritis), CD25; $n = 27$ analysis (14 SpA, 10 RA and two reactive arthritis), GITR; $n = 9$ (five SpA and four RA), CTLA-4; $n = 13$ (10 SpA and three RA) and for CD62L; $n = 21$ (14 SpA, five RA and two reactive arthritis). Paired SF and PB samples were used for the IL-1R1 stainings, $n = 14$ (nine SpA and five RA). For the cytokine staining experiments, SF samples from six patients diagnosed with SpA were analysed. Patients included in the cytokine and IL-1R experiments were also included in the phenotypical analysis of T_{reg} expression markers. With regard to therapy, 33 patients were receiving disease-modifying anti-rheumatic drugs (DMARDs), such as methotrexate or sulphasalazine, cortisone or anti-tumour necrosis factor (TNF) treatment or a combination of these drugs, four patients were receiving CTLA-4 agonist therapy (abatacept) and nine were untreated. The study was performed under informed consent and after ethical approval from the Karolinska University Hospital.

Phenotypical flow cytometry

Single-cell suspensions from PB and SF mononuclear cells were surface-stained with the following antibodies in different combinations: anti-IL-1R1-phycoerythrin (PE) (R&D Systems, Minneapolis, MN, USA), anti-CD62L-ECD (Beckman Coulter, Brea, CA, USA), anti-CD25 peridinin chlorophyll-cyanin (PerCP-CY)5·5 or PE-Cy7, anti-CCR6 PerCP-CY5·5, anti-CD4 PerCP-CY5·5 or PE-Cy7,

anti-CD14-allophycocyanin (APC)-Cy7 (Becton Dickinson, Franklin Lakes, NJ, USA), anti-CCR7, -CXCR3, or -CCR4 Brilliant Violet 421 (Biolegend, San Diego, CA, USA) anti-CD3 Cascade Yellow (Dako, Glostrup, Denmark) or Brilliant Violet 510 (Biolegend) and GITR PE (Becton Dickinson). Cells were incubated on ice in the dark for 30 min. Cells were then washed twice in phosphate-buffered saline (PBS) supplemented with 1% human male AB serum for the first wash, and only PBS the second time. Cells were fixed and permeabilized for 30 min on ice in the dark using FoxP3 intranuclear staining kit (eBioscience, San Diego, CA, USA). Cells were then stained for Ki67-Alexa Fluor 488 (Becton Dickinson), CTLA-4-PE (Becton Dickinson), Helios-Alexa Fluor 647 or Helios-Alexa Fluor 488 (BioLegend) and anti-FoxP3-Pacific blue or anti-FoxP3-Alexa Fluor 647 (clone 206D; BioLegend). LIVE/DEAD fixable Near-IR (Invitrogen, Carlsbad, CA, USA) was used in some stainings to exclude dead cells.

Cells were acquired on a Gallios instrument (Beckman Coulter) and data were compensated and analysed with FlowJo software (TreeStar, Inc., Ashland, OR, USA).

Intracellular cytokine staining

Ficoll-separated SF cells from six patients diagnosed with arthritis were cultured in RPMI-1640 supplemented with 5% heat-inactivated AB autologous serum, penicillin (100 U/ml), streptomycin (100 μg/ml), 2 mM L-glutamine and 10 mM HEPES. The cells were cultured in the presence or absence of plate-bound anti-CD3 (1·0 μg/ml clone OKT-3) for 16 h. Brefeldin A (10 μg/ml) was added in the last 5 h of the stimulation. Cells were harvested, washed and stained for surface markers using the following fluorochrome conjugated antibodies, anti-CD3-Cascade yellow (Dako) and anti-CD4-APC-Cy7 (Becton Dickinson). Cells were washed twice, fixed and permeabilized using FoxP3 fixation/permeabilization solutions and buffers for FoxP3 staining (eBioscience). Briefly, FoxP3 fixation/permeabilization solution was added to the cells and incubated for 30 min on ice in the dark followed by two washes with permeabilization buffer. Cells were then stained for IL-10-PE (clone P3; eBioscence,), IFN-γ-PECy7 (clone B27; BD), TNF-PerCp-Cy5·5 (Biolegend), FoxP3-Pacific blue (clone 206D; Biolegend) or isotype-matched control antibody.

Gating strategies

Cells were gated as follows: lymphocytes were identified using forward- and side-scatter properties, cell doublets and $CD14^+$ and dead cells were excluded. The continuous phenotypical analysis was performed on $CD14^-CD3^+CD4^+FoxP3^+Helios^+$ or $CD14^-CD3^+CD4^+FoxP3^+Helios^-$ cells. IL-1R1, CD62L, CTLA-4, Ki67, CD25, GITR, CCR7, CXCR3, CCR4, CCR6, IFN-γ, IL-10 and TNF were displayed in dot-plots against CD4. Analysis of the different Helios and FoxP3 subpopulations was performed as shown in the dot-plots in Fig. 1a,b.

TSDR methylation analysis

PB and SF $CD3^+CD4^+$ cells from male SpA patients ($n = 5$) were sorted into $Helios^+FoxP3^-$, $Helios^+FoxP3^+$, $Helios^-FoxP3^+$ and $Helios^-FoxP3^-$ T cells. Sorted cells were > 95% pure for all sorted subpopulations upon post-sort reanalysis. Genomic DNA was isolated according to the manufacturer's instructions using the DNeasy blood

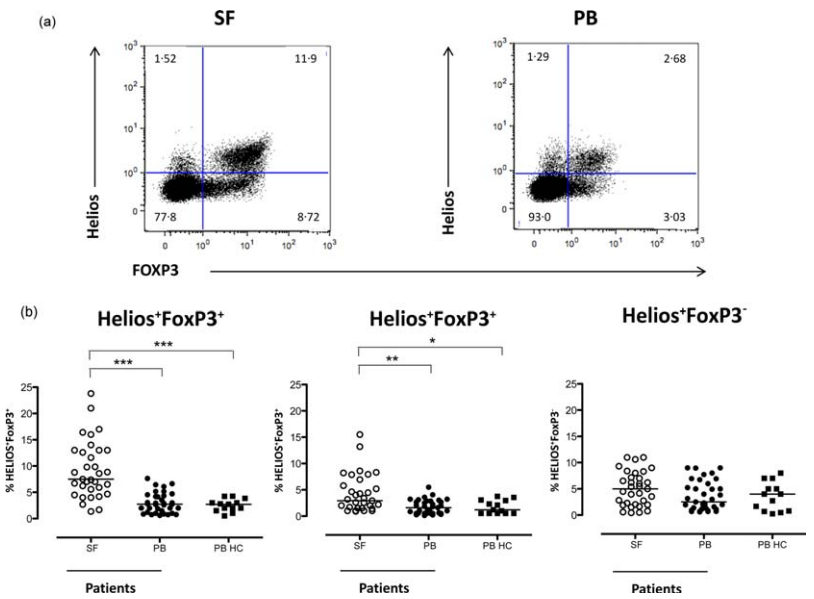

Fig. 1. The $Helios^+FoxP3+$ and $Helios^-FoxP3^+$ T cell populations are enriched in synovial fluid (SF) compared to blood from patients with inflammatory arthritis. Flow cytometric analysis of Helios and FoxP3 expression was performed in SF and peripheral blood (PB) of patients with inflammatory arthritis, and blood from healthy controls (HC). Analysis of the distribution of Helios and FoxP3 expression was performed on $CD14^-CD3^+CD4^+$ T lymphocytes (defined by forward- and side-scatter). Representative dot-plots of Helios and FoxP3 stainings are shown for SF and PB (a). The graphs summarize the respective frequencies of $Helios^+FoxP3^+$, $Helios^-FoxP3^+$ and $Helios^+FoxP3^-$ (b) in $CD3^+CD4^+$ T cell subpopulations in SF ($n = 33$) and PB ($n = 35$) from patients and PB from HC ($n = 11$) (for diagnosis status of the study objects included please see the Materials and methods section). Data were analysed using the Kruskal–Wallis test with Dunn's multiple-comparison post test, $^{***}P < 0{\cdot}001$, $^{**}P < 0{\cdot}005$ and $^{*}P < 0{\cdot}05$.

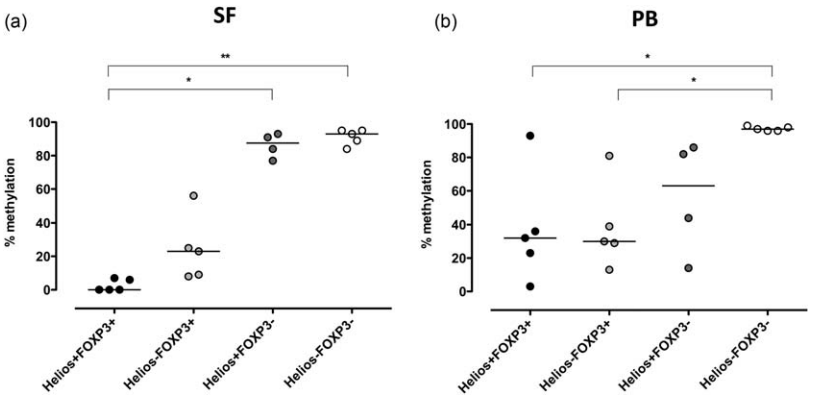

Fig. 2. Synovial Helios$^+$FoxP3+ T cells display the highest demethylated T_{reg}-specific demethylated region (TSDR) of the two T_{reg} subsets. Helios$^+$FoxP3$^+$, Helios$^-$FoxP3$^+$, Helios$^+$FoxP3$^-$ and Helios$^-$FoxP3$^-$ T cells were sorted from synovial fluid (a) and peripheral blood (b) of five patients with ankylosing spondylitis (SpA). The degree of methylation in the FoxP3 gene locus is depicted for the different subsets. Kruskal–Wallis test with Dunn's multiple-comparison test $^{**}P < 0{\cdot}005$ and $^{*}P < 0{\cdot}05$.

and tissue kit (Qiagen, Valencia, CA, USA). DNA methylation of 15 CPGs within the TSDR (Amplicon 5) were performed by bisulphite sequencing, as described elsewhere [30], and were performed by Epiontis (Berlin, Germany).

Statistical analysis

Data analysis was performed using GraphPad Prism version 5·0 (GraphPad). The Kruskal–Wallis test with Dunn's multiple comparison post-test was used when comparing more than two groups. Wilcoxon's signed-rank test was used to evaluate statistics between paired patient samples and Mann–Whitney *U*-test when comparing data in non-paired samples. Correlation between data points was carried out using Spearman's correlation analysis

Results

Helios$^+$FoxP3$^+$ T cells is the most abundant T_{reg} subset in the rheumatic joint

Four different subsets can be distinguished after gating CD4$^+$ T cells based on expression of FoxP3 and Helios (Fig. 1a). We found a significant enrichment of both Helios$^+$FoxP3$^+$ ($P < 0{\cdot}0001$) and Helios$^-$FoxP3$^+$CD4$^+$ T cells ($P < 0{\cdot}005$) (Fig. 1b) in SF compared to PB. However, the Helios$^+$FoxP3$^+$ T_{regs} were the most prevalent subset in SF, median 7·5% (range 1·4–23·8%) of all CD4$^+$ T cells. Helios was also expressed in the absence of FoxP3, but in this context no significant differences were found between the compartments analysed or between patients and healthy controls. For all these analyses, overlapping frequencies were seen for the different patient groups included in the study (data not shown).

Synovial Helios$^+$FoxP3$^+$ T cells display the most demethylated TSDR region of the CD4 subsets in the joint

As functional studies on Helios$^-$FoxP3$^+$ T cells and Helios$^+$FoxP3$^+$ T cells cannot be performed due to the intranuclear expression of both transcription markers, epigenetic profiling of the TSDR can be used as an indication for T_{reg} functionality. Therefore, we analysed the methylation status of the T_{reg}-specific TSDR on fixed [31] and sorted FoxP3- and Helios-stained CD4$^+$ T cells derived from PB and SF of five male SpA patients. As shown in Fig. 2a, sorted synovial Helios$^+$FoxP3$^+$ T cells revealed a fully demethylated TSDR with a median methylation of 0% (range 0–7%), while Helios$^-$FoxP3$^+$ T cells showed a median methylation of 23% (range 8–56%). In contrast, Helios$^+$FoxP3$^-$ and Helios$^-$FoxP3$^-$ T cells showed close to full methylation in this region with a median of 87·5% (range 77–93%) and 93% (range 84–95%), respectively. The picture for PB was less homogeneous, and here Helios$^+$ and Helios$^-$FoxP3$^+$ cells had comparable levels of demethylation, with a median methylation of 32% (range 3–93%) and 30% (range 13–81%), respectively (Fig. 2b).

Synovial Helios$^+$FoxP3$^+$ T cells display the most classical T_{reg} phenotype

To deduce phenotypically which FoxP3$^+$ T cell subset best represented the classical definition of T_{regs}, we investigated whether there were any differences in the expression of well-known T_{reg} markers.

The frequency of CD25-expressing cells varied within both T_{reg} subpopulations in SF and in PB. Nevertheless, in both these compartments we observed a significantly higher frequency of CD25^{high} CD4$^+$ T cells in the Helios$^+$FoxP3$^+$ subpopulation compared to the Helios$^-$FoxP3$^+$ counterpart, in SF $P < 0{\cdot}005$ and in PB $P < 0{\cdot}005$ (Fig. 3a,b).

Next we analysed the expression patterns of GITR, CTLA-4 and L-selectin lymph node homing receptor CD62L. All these three proteins have been associated with functional properties of T_{regs} [32–36]. The frequencies of GITR-positive cells were equally high in both FoxP3 subsets in the inflamed joints and also overall higher compared to blood, where only a low frequency of GITR expression was observed (Fig. 3a,b). The majority of the T_{reg} cells in the inflamed joints stained positive for CTLA-4 and the frequency of CTLA-4-positive Helios$^+$ and Helios$^-$FoxP3$^+$ cells was significantly higher compared to the FoxP3$^-$CD4$^+$ T cells, $P < 0{\cdot}001$ and $P < 0{\cdot}005$, respectively (Fig. 3a). In contrast, the CTLA-4 expression on FoxP3$^+$ cells in blood showed

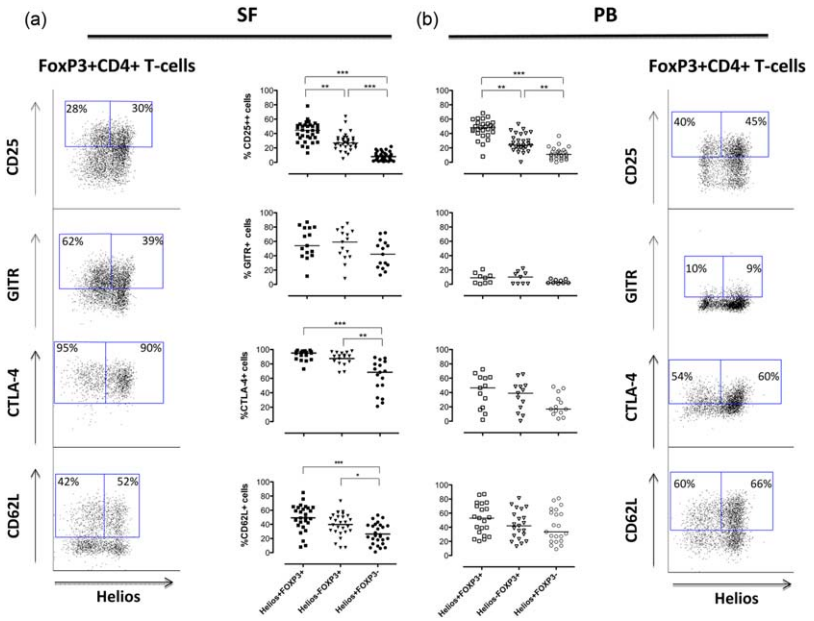

Fig. 3. The interleukin (IL)-2 alpha-receptor CD25 is expressed more frequently on Helios$^+$FoxP3+ compared to Helios$^-$FoxP3$^+$CD4$^+$ T cells. A comparison of the different subpopulations expression pattern, in patient-derived synovial fluid (SF) (a) and peripheral blood (PB) (b), is shown for the following cell-surface markers. CD25 (SF $n = 33$, PB $n = 27$), glucocorticoid-induced tumour necrosis factor (TNF) receptor family-related gene (GITR) (SF $n = 15$, PB $n = 9$), cytotoxic T lymphocyte antigen (CTLA)-4 (SF $n = 17$, PB $n = 13$) and CD62L (SF $n = 27$, PB $n = 21$). Analysis of the distribution of the different T_{reg} markers was performed on CD14$^-$CD3$^+$CD4$^+$ T lymphocytes (defined by forward- and side-scatter) (for diagnosis status of the study objects included please see the Materials and methods section). The dot-plots display staining pattern and gating strategies for these markers in FoxP3$^+$CD4$^+$CD3$^+$ cells in SF (left column) and PB (right column). Data was analysed using the Kruskal–Wallis test with Dunn's multiple-comparison post-test, significance: $^{***}P < 0{\cdot}001$, $^{**}P < 0{\cdot}005$ and $^{*}P < 0{\cdot}05$.

extensive heterogeneity (Fig. 3b). Finally, the expression of CD62L was somewhat variable between patients and showed a similar expression pattern on T_{regs} and FoxP3$^-$ cells in both SF and PB (Fig. 3a,b). We did not observe any significant differences in the frequencies of cells positive for these T_{reg} markers between patient groups except for GITR, which was less expressed on synovial Helios$^+$ and Helios$^-$FoxP3$^+$ cells in RA compared to SpA (data not shown).

Helios$^+$FoxP3$^+$ T cells do not produce IFN-γ or IL-10

Recent studies have proposed that T_{regs} are plastic and may be able to secrete proinflammatory cytokines, but there is still a controversy regarding whether they also lose their regulatory capacity [37]. In a previous study we demonstrated that synovial CD4$^+$FoxP3$^+$ T cells were poor producers of proinflammatory cytokines [24]; however, a small production could be observed, and we now revisited this issue in the context of Helios expression. As seen in Fig. 4, Helios$^+$FoxP3$^+$ T cells did not produce IFN-γ, and hardly any TNF. In contrast, the Helios$^-$FoxP3$^+$ subpopulation expressed both cytokines and even displayed the highest frequencies of TNF-positive cells of all tested subsets (Fig. 4a,b).

IL-10 is a cytokine often assigned to exhibit immunosuppressive properties, but which is also important for B cell activation/propagation [38,39]. T_{regs} from mucosal sites have been demonstrated to secrete this cytokine [40]. However, in our study, the joint-derived Helios$^+$FoxP3$^+$ T_{reg} cells also failed to produce IL-10, while the Helios$^-$FoxP3$^+$ subpopulation was able to produce this cytokine (Fig. 4c).

Synovial Helios$^+$FoxP3$^+$ T cells have a higher proliferation rate compared with Helios$^-$FoxP3$^+$ T cells

As mentioned, Helios is also regarded currently as a marker of T cell activation and proliferation. To this end we included Ki67, a marker of proliferation, in our analysis and found that the highest frequency of CD4$^+$ T cells in cell cycle was observed among the joint-derived Helios$^+$FoxP3$^+$ cells (median 27%, range 13–68%), while the Helios$^-$FoxP3$^+$ and Helios$^+$FoxP3$^-$ T cells displayed similar levels of Ki67 expression, with a median of 21% Ki67-positive cells, range 3–49% for Helios$^-$FoxP3$^+$ and 7·5–37% for the Helios$^+$FoxP3$^-$ subset. This pattern was consistent in both compartments, but with the highest frequencies of proliferating Ki67$^+$ cells in SF (Fig. 5). Given these data, we next asked if the observed higher frequency of synovial Helios$^+$FoxP3$^+$ T cells in the cell cycle could explain the observed accumulation of these cells. However, no such tendencies were found (data not shown).

Chemokine and cytokine receptor expression in the Helios$^{+/-}$FoxP3$^{+/-}$ T cell subsets

To be able to test whether or not the joint-derived Helios$^-$FoxP3$^+$ T cells are suppressive, a surface marker, which could enrich for Helios$^-$FoxP3$^+$ T cells would be of great value. Given the production of proinflammatory cytokines in the Helios$^-$FoxP3$^+$ T cells we next analysed

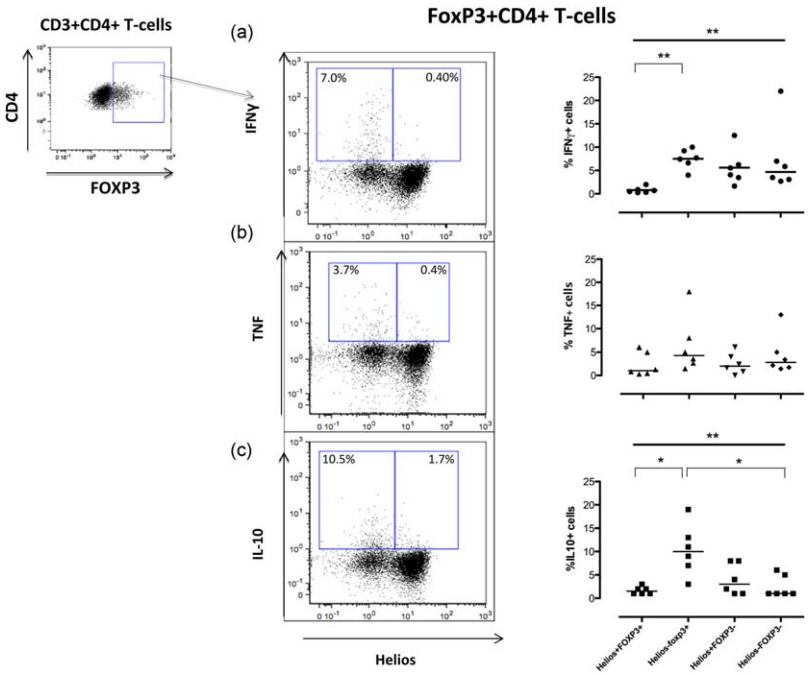

Fig. 4. Helios$^-$FoxP3$^+$ but not Helios$^+$FoxP3$^+$ T cells produce interferon (IFN)-γ, tumour necrosis factor (TNF) and interleukin (IL)-10. Synovial fluid cells from five patients [ankylosing spondylitis (SpA)] were stimulated with plate-bound a-CD3 for 16 h, the last 5 h in the presence of brefeldin A. Cells were harvested and analysed by flow cytometry for cytokines. Representative dot-plots show CD14$^-$CD3$^+$CD4$^+$FoxP3$^+$ T cells plotted against Helios and the respective cytokine [i.e. IFN-γ (a), TNF (b) and IL-10 (c)]. Summary graph for IFN-γ is depicted in (a), for TNF in (b) and IL-10 in (c). Data were analysed using the Kruskal–Wallis test together with Dunn's multiple-comparision post-test, $P < 0{\cdot}001$, $^{**}P < 0{\cdot}005$ and $^{*}P < 0{\cdot}05$.

the expression pattern of chemokine receptors associated with T helper type 1 (Th1) (CXCR3), Th17 (CCR6) and Th2 (CCR4). Overall, in both SF and PB, most chemokine receptors were expressed similarly in the FoxP3 subsets (as well as in the FoxP3-negative cells), with the exception of an enhanced expression of CCR4 on synovial T_{reg} which, however, was independent of Helios expression (Supporting information, Fig. S1).

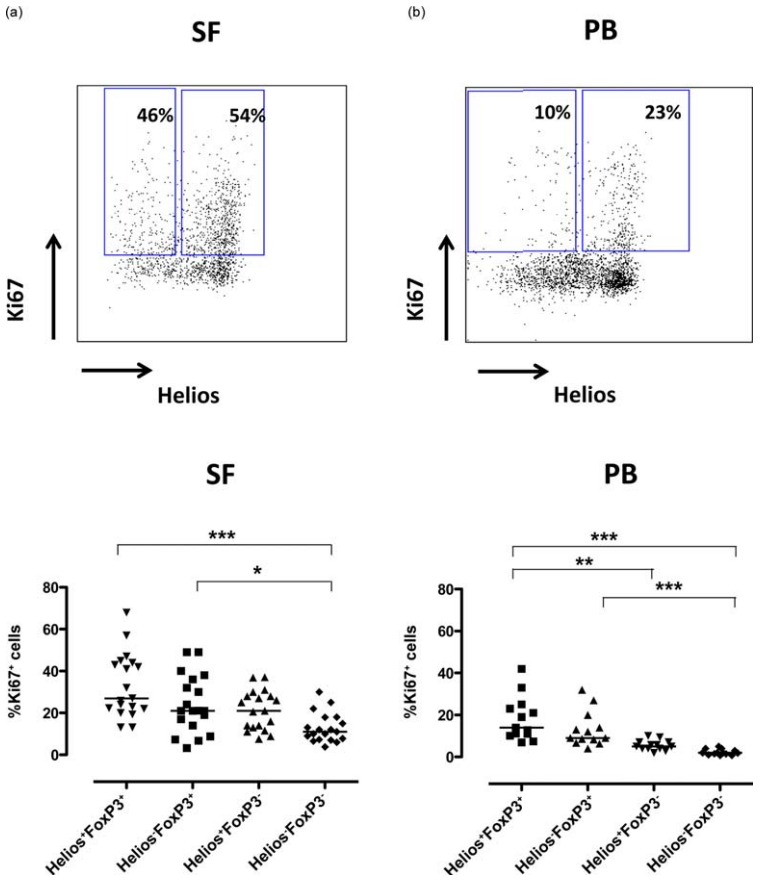

Fig. 5. Synovial Helios$^+$FoxP3$^+$ T cells displayed the highest frequency of cycling cells. Mononuclear cells from inflamed joints [synovial fluid (SF)] ($n = 19$) [13 ankylosing spondylitis (SpA), three rheumatoid arthritis (RA), three juvenile arthritis (JIA)] and from peripheral blood (PB) ($n = 13$) (10 SpA, three RA) of arthritis patients were analysed by flow cytometry for the proliferation marker Ki67. CD14$^-$ single cells were gated via CD3 and CD4 and subsequently Helios$^+$FoxP3$^+$ and Helios$^-$FoxP3$^+$ T cells positive for Ki67 are depicted. The dot-plots show representative Ki67 and Helios stainings of CD3$^+$CD4$^+$FoxP3$^+$ cells in SF (a) and PB (b) from patients. Summary graphs of the proliferation in the different Helios FoxP3 subpopulations are shown for SF (a) and PB (b). The proliferation data were compared using the Kruskal–Wallis test together with Dunn's multiple-comparision post-test, significance: $^{***}P < 0{\cdot}001$, $^{**}P < 0{\cdot}005$ and $^{*}P < 0{\cdot}05$.

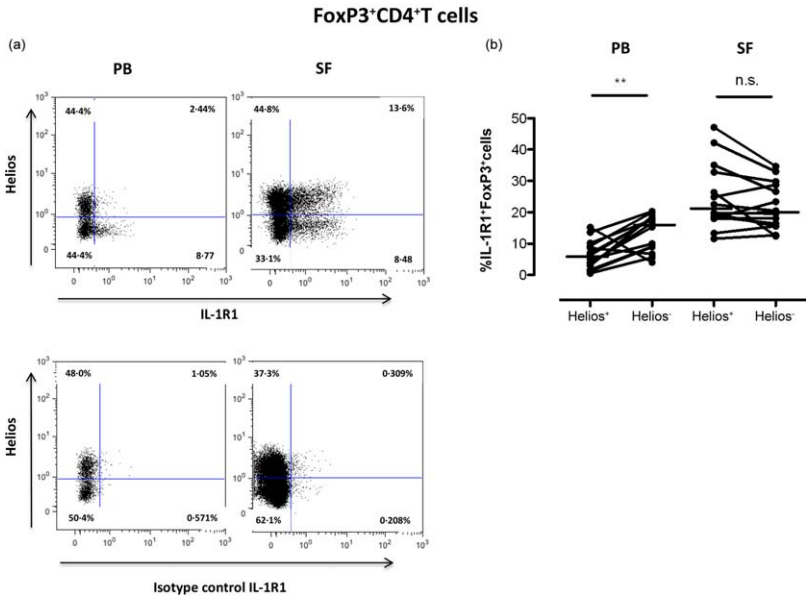

Fig. 6. Expression of interleukin (IL)-1R1 in synovial cells is restricted to FoxP3$^+$CD25^{++}CD4 T cells. (a) Representative stainings of the distribution of IL-1R1 expression on Helios$^+$ and Helios$^-$ FoxP3$^+$ T cells (upper panel) and isotype control of the IL-1R1 antibody (lower panel) in peripheral blood (PB) and synovial fluid (SF). (b) The graph summarizes the frequencies of IL-1R1-positive Helios$^-$ and Helios$^+$FoxP3$^+$ cells in PB and SF. (c) The dot-plots show the distribution of IL-1R1 expression on CD4$^+$ T cells in PB and SF, respectively, and the graph (d) summarizes the frequencies of IL-1R1$^+$FoxP3$^+$ T cells in PB and SF (c). Representative dot-plots and summary graphs of the distribution of CD25 and IL-1R1 expression in the FoxP3 population are shown in (e) (PB) and (f) (SF). All stainings were performed on paired PB and SF samples from 14 patients diagnosed with inflammatory arthritis [nine ankylosing spondylitis (SpA) and five rheumatoid arthritis (RA)]. Data were compared using the Wilcoxon's signed-rank test, $^{**}P < 0{\cdot}001$ and $^{***}P < 0{\cdot}0001$.

IL-1R1 expression is elevated significantly on both Helios$^+$ and Helios$^-$ synovial T_{regs}

Of note, a recent study demonstrated that the chemokine receptor CCR7 in combination with the cytokine receptor IL-1R1 was restricted largely to the Helios-negative subpopulation of FoxP3$^+$ T cells [20]. Hence, we analysed if these markers could also be applied to Helios$^-$FoxP3$^+$ T cells from patients with inflammatory arthritis. Using this combination, the frequency of Helios$^-$FoxP3$^+$ cells in PB increased from a median of 30% (range 20–50%) when gated only via CD25 to 70% (range 25–77%) when including CCR7 and IL-1R1. Indeed, even in the absence of CCR7, gating via IL-1R1 expression increased the frequency of Helios$^-$FoxP3$^+$ T cells from 22% (range 12·6–34%) up to a median 55% (range 17·9–84%) (Supporting information, Fig. S2).

In contrast, co-expression of IL-1R1 and CCR7 on CD25 bright T cells from SF did not enrich for Helios$^-$FoxP3$^+$ cells (Supporting information, Fig. S2). IL-1R1 expression was prominent in the joint-derived FoxP3 cells, but was distributed equally between Helios$^+$ and Helios$^-$ T_{regs}, medians 21% (range 11·5–47%) and 20% (range 12·5–35%), respectively (Fig. 6a,b). In contrast, the FoxP3$^-$ T cells hardly expressed IL-1R1 at all (Fig. 6c). On average, more than 20% of the joint-derived FoxP3$^+$ T cells expressed IL-1R1, and this was significantly greater than in PB (Fig. 6d). The IL-1R1 expression coincided strongly with CD25 expression both in SF and in PB, even though this subset was less pronounced in the circulation (Fig. 6e,f). Moreover, the expression pattern of IL-1R1 was similar in both RA and SpA patients (Supporting information, Fig. S3).

Discussion

Helios, a transcription factor belonging to the Ikaros family, has been studied extensively in the context of human T_{reg} in health and disease [14,16–20,36]. We have a long-standing interest in the rheumatic joint, a site of inflammation characterized by extensive cell influx and proliferation and where, in addition to activated memory effector T cells, T_{regs} are also enriched significantly compared to PB [23]. Indeed, there is a growing appreciation that tissue T_{regs} are different from T_{regs} in the circulation [41], and we can contribute to this field by our parallel analyses of patient samples from PB and SF. Herein we have focused on Helios and Helios-related phenotypes in the context of tissue T_{reg} from rheumatic joints of patients with RA and SpA. These two diseases have overlapping manifestations and similar treatment strategies, but also display different underlying aetiologies [42,43]. Hereby, the commonalities we find are likely to be driven by the local inflammatory environment, and not by the initiating factors for disease occurrence.

We found that Helios is expressed more abundantly in SF compared to PB. The median frequency of Helios expression in the entire CD4 T cell population was 13% in SF compared to 7% in PB. This was not entirely unexpected, as Helios has been linked to T cell activation and proliferation [16,17], and prompted us to dissect the synovial T_{reg} compartment in the context of Helios. Both

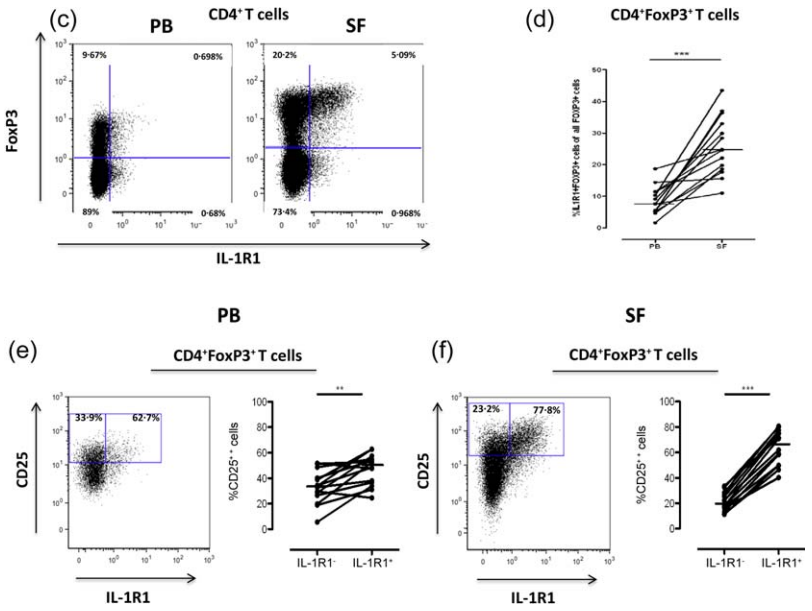

Fig. 6. *Continued*

Helios$^+$ and Helios$^-$FoxP3$^+$ T_{regs} were enriched in SF, with the Helios$^+$FoxP3$^+$ cells being the most prominent subset.

In contrast, no enrichment of Helios$^+$FoxP3$^+$ or Helios$^-$FoxP3$^+$ CD4 T cells was found in PB of patients compared to healthy donors. This finding is supported by results from a recent study, where enrichment of Helios$^+$ FoxP3$^+$ T cells could not be observed in the circulation of RA and systemic sclerosis patients, while patients with active systemic lupus erythematosus (SLE) displayed elevated levels [19].

In the present study, when analysing the phenotype of Helios$^+$ and Helios$^-$FoxP3$^+$ T cells in patients with inflammatory arthritis, the compartment (i.e. PB *versus* SF) was more important for the outcome of the analysis than diagnosis (RA *versus* SpA), emphasizing the impact of the local inflammatory environment. The largest difference in T_{reg} phenotype, between the inflamed joints and the circulation, was seen for the expression of GITR and CTLA-4. In SF, both CTLA-4 and GITR expression was highly up-regulated on FoxP3$^+$ T_{reg} cells independently of Helios expression. This data set suggests that GITR and CTLA-4 are central to the inflammatory tissue T_{reg} phenotype. Although we could not perform functional studies of the Helios T_{reg} subsets, we analysed methylation levels of the TSDR of both blood- and joint-derived cells. This represents a good proxy for T_{reg} function [30,44] and, again, the SF samples were different to those from PB, with the FoxP3$^+$ T cell subsets demonstrating more substantial demethylation in the joint; in particular, the Helios$^+$ FoxP3$^+$ demonstrated a robust T_{reg} phenotype.

With regard to differences between the Helios$^+$ and the Helios$^-$FoxP3 T_{reg} subsets, a higher frequency of CD25-expressing cells was observed, both in PB and SF, in the Helios$^+$FoxP3$^+$ cell population. Additionally, the joint-derived Helios$^+$FoxP3$^+$ T_{regs} did not produce IFN-γ, TNF or IL-10 following *in-vitro* activation while the Helios$^-$ FoxP3$^+$ counterpart did. These data are also in line with findings from other groups [18,19,36]. Himmel *et al.* demonstrated that cloned Helios$^+$ and Helios$^-$ T_{reg} from healthy donors expressed similar cell surface markers, but differed in their capability to produce cytokines and both subsets were still suppressive [18]. Supported by our epigenetic analyses, our data imply that in the rheumatic joint both FoxP3 subsets could also contribute to alleviating the inflammatory pressure. Furthermore, the chemokine receptor CCR4 has been implicated previously in suppressive capacity of effector regulatory T cells [45,46], and in our SF samples this marker was elevated equally on both Helios$^+$ and Helios$^-$FoxP3 T cells, again suggesting the suppressive capacity of both cell subtypes.

To be able to investigate the possible differences in regulatory properties of Helios$^+$FoxP3$^+$ and Helios$^-$FoxP3$^+$ T cells it would be of great value to find a robust cell surface marker which would distinguish these two cell subpopulations from each other. A recent study in humans demonstrates that blood-derived T_{reg} cells which co-express IL-1R1 and CCR7 are enriched (but not exclusive) for Helios$^-$FoxP3$^+$ cells and also that these IL-1R1-expressing Helios$^-$FoxP3$^+$ T_{regs} lost their suppressive capacity in the presence of IL-1β [20]. We could confirm that the combination of IL-1R1 and CCR7 expression was useful in blood. However, in the inflammatory milieu of the rheumatic joint, these markers could not enrich for Helios$^-$FoxP3$^+$ T cells. Instead, we observed an increased expression of IL-1R1 on synovial T cells, which was almost exclusive for CD25^{high} FoxP3$^+$ cells, but without distinguishing Helios$^+$ from Helios$^-$ T_{reg} cells. The expression pattern of IL-1R1 was similar in patients diagnosed with RA and SpA, suggesting that the up-regulation of IL-1R1 on T_{regs} is a common feature in an inflammatory milieu. The function of

IL-1R1 on regulatory T cells is not fully known, but has been suggested to be linked to sensing infectious/inflammatory signals, proliferation and expansion in order to control the inflammation. [47,48]. We and others have shown previously that joint-derived T_{regs} have suppressive capacity *in vitro* [23,24], but it is possible that in the presence of IL-1β, which is present in the rheumatic joint [49], regulatory T cells expressing the receptor for this cytokine could transiently lose their suppressive activity.

In conclusion, the dissection of the synovial FoxP3$^+$ T cell population in combination with Helios supports and extends the notion of T_{reg} accumulation in the joint. Both Helios$^+$ and Helios$^-$FoxP3 T cells in the joint have the appearance of classical regulatory T cells, the major differences being that the Helios$^+$ T_{reg} could be regarded as the most robust (non-plastic) subset due to their consistent epigenetic feature and absence of cytokine production. The Helios$^-$ T_{reg} subset also displays many features of classical synovial T_{regs}, including high expression of CTLA-4, but with the capacity of secreting cytokines. We also observed a general up-regulation of IL-1R1 on synovial T_{reg} that did not coincide with any of the Helios subsets. These different facets of tissue T_{regs} deserve closer examination, in the context of which the T_{reg} phenotype would be the most interesting for future therapeutic approaches.

Acknowledgements

The authors thank the staff and patients at the Rheumatology Clinic of Karolinska University Hospital and the Rheumatology Research laboratory, especially Eva Jemseby, Gull-Britt Almgren and Julia Boström for organizing the sampling, storage and administration of biomaterial and Annika van Vollenhoven for excellent cell sorting. The work was supported by grants from the Swedish Association against Rheumatism, the King Gustaf V 80 year Foundation, the Swedish Research Council, the TREG CENTER consortia, the EU FP7 project Masterswitch (HEALTH-F2-2008-223404) and the IMI JU funded project BTCure 115142-2.

Disclosures

The authors declare no financial or commercial conflicts of interest.

References

1 Sakaguchi S, Sakaguchi N, Asano M, Itoh M, Toda M. Immunologic self-tolerance maintained by activated T cells expressing IL-2 receptor alpha-chains (CD25). Breakdown of a single mechanism of self-tolerance causes various autoimmune diseases. J Immunol 1995; **155**:1151–64.

2 Wehrens EJ, Prakken BJ, van Wijk F. T cells out of control–impaired immune regulation in the inflamed joint. Nat Rev Rheumatol 2013; **9**:34–42.

3 Hori S, Nomura T, Sakaguchi S. Control of regulatory T cell development by the transcription factor Foxp3. Science 2003; **299**:1057–61.

4 Zheng Y, Rudensky AY. Foxp3 in control of the regulatory T cell lineage. Nat Immunol 2007; **8**:457–62.

5 Zahorsky-Reeves JL, Wilkinson JE. The murine mutation scurfy (sf) results in an antigen-dependent lymphoproliferative disease with altered T cell sensitivity. Eur J Immunol 2001; **31**:196–204.

6 Bennett CL, Christie J, Ramsdell F *et al.* The immune dysregulation, polyendocrinopathy, enteropathy, X-linked syndrome (IPEX) is caused by mutations of FOXP3. Nat Genet 2001; **27**: 20–1.

7 Godfrey VL, Wilkinson JE, Russell LB. X-linked lymphoreticular disease in the scurfy (sf) mutant mouse. Am J Pathol 1991; **138**: 1379–87.

8 Wildin RS, Ramsdell F, Peake J *et al.* X-linked neonatal diabetes mellitus, enteropathy and endocrinopathy syndrome is the human equivalent of mouse scurfy. Nat Genet 2001; **27**:18–20.

9 Walker LS, Sansom DM. Confusing signals: recent progress in CTLA-4 biology. Trends Immunol 2015; **36**:63–70.

10 Waterhouse P, Penninger JM, Timms E *et al.* Lymphoproliferative disorders with early lethality in mice deficient in CTLA-4. Science 1995; **270**:985–8.

11 Tivol EA, Borriello F, Schweitzer AN, Lynch WP, Bluestone JA, Sharpe AH. Loss of CTLA-4 leads to massive lymphoproliferation and fatal multiorgan tissue destruction, revealing a critical negative regulatory role of CTLA-4. Immunity 1995; **3**:541–7.

12 Schubert D, Bode C, Kenefeck R *et al.* Autosomal dominant immune dysregulation syndrome in humans with CTLA4 mutations. Nat Med 2014; **20**:1410–6.

13 Durand C, Kerfourn F, Charlemagne J, Fellah JS. Identification and expression of Helios, a member of the Ikaros family, in the Mexican axolotl: implications for the embryonic origin of lymphocyte progenitors. Eur J Immunol 2002; **32**:1748–52.

14 Thornton AM, Korty PE, Tran DQ *et al.* Expression of Helios, an Ikaros transcription factor family member, differentiates thymic-derived from peripherally induced Foxp3+ T regulatory cells. J Immunol 2010; **184**:3433–41.

15 Akimova T, Beier UH, Wang L, Levine MH, Hancock WW. Helios expression is a marker of T cell activation and proliferation. PLOS ONE 2011; **6**:e24226.

16 Gottschalk RA, Corse E, Allison JP. Expression of Helios in peripherally induced Foxp3+ regulatory T cells. J Immunol 2012; **188**:976–80.

17 Getnet D, Grosso JF, Goldberg MV *et al.* A role for the transcription factor Helios in human CD4(+)CD25(+) regulatory T cells. Mol Immunol 2010; **47**:1595–600.

18 Himmel ME, MacDonald KG, Garcia RV, Steiner TS, Levings MK. Helios+ and Helios– cells coexist within the natural FOXP3+ T regulatory cell subset in humans. J Immunol 2013; **190**:2001–8.

19 Alexander T, Sattler A, Templin L *et al.* Foxp3+ Helios+ regulatory T cells are expanded in active systemic lupus erythematosus. Ann Rheum Dis 2013; **72**:1549–58.

20 Raffin C, Pignon P, Celse C, Debien E, Valmori D, Ayyoub M. Human memory Helios- FOXP3+ regulatory T cells (Tregs) encompass induced Tregs that express Aiolos and respond to IL-1beta by downregulating their suppressor functions. J Immunol 2013; **191**:4619–27.

21 Garlanda C, Dinarello CA, Mantovani A. The interleukin-1 family: back to the future. Immunity 2013; **39**:1003–18.
22 Mottonen M, Heikkinen J, Mustonen L, Isomaki P, Luukkainen R, Lassila O. CD4+ CD25+ T cells with the phenotypic and functional characteristics of regulatory T cells are enriched in the synovial fluid of patients with rheumatoid arthritis. Clin Exp Immunol 2005; **140**:360–7.
23 Michels-van Amelsfort JM, Walter GJ, Taams LS. CD4+CD25+ regulatory T cells in systemic sclerosis and other rheumatic diseases. Expert Rev Clin Immunol 2011; **7**:499–514.
24 Herrath J, Muller M, Amoudruz P *et al.* The inflammatory milieu in the rheumatic joint reduces regulatory T-cell function. Eur J Immunol 2011; **41**:2279–90.
25 van Amelsfort JM, van Roon JA, Noordegraaf M *et al.* Proinflammatory mediator-induced reversal of CD4+,CD25+ regulatory T cell-mediated suppression in rheumatoid arthritis. Arthritis Rheum 2007; **56**:732–42.
26 Valencia X, Stephens G, Goldbach-Mansky R, Wilson M, Shevach EM, Lipsky PE. TNF downmodulates the function of human CD4+CD25hi T-regulatory cells. Blood 2006; **108**:253–61.
27 Ondondo B, Jones E, Godkin A, Gallimore A. Home sweet home: the tumor microenvironment as a haven for regulatory T cells. Front Immunol 2013; **4**:197.
28 Girardin A, McCall J, Black MA *et al.* Inflammatory and regulatory T cells contribute to a unique immune microenvironment in tumor tissue of colorectal cancer patients. Int J Cancer 2013; **132**:1842–50.
29 Schneider A, Rieck M, Sanda S, Pihoker C, Greenbaum C, Buckner JH. The effector T cells of diabetic subjects are resistant to regulation via CD4+ FOXP3+ regulatory T cells. J Immunol 2008; **181**:7350–5.
30 Baron U, Floess S, Wieczorek G *et al.* DNA demethylation in the human FOXP3 locus discriminates regulatory T cells from activated FOXP3(+) conventional T cells. Eur J Immunol 2007; **37**:2378–89.
31 Hansmann L, Schmidl C, Boeld TJ *et al.* Isolation of intact genomic DNA from FOXP3-sorted human regulatory T cells for epigenetic analyses. Eur J Immunol 2010; **40**:1510–2.
32 Walker LS. Treg and CTLA-4: two intertwining pathways to immune tolerance. J Autoimmun 2013; **45**:49–57.
33 Ermann J, Hoffmann P, Edinger M *et al.* Only the CD62L+ subpopulation of CD4+CD25+ regulatory T cells protects from lethal acute GVHD. Blood 2005; **105**:2220–6.
34 Goudy KS, Johnson MC, Garland A *et al.* Reduced IL-2 expression in NOD mice leads to a temporal increase in CD62Llo FoxP3+ CD4+ T cells with limited suppressor activity. Eur J Immunol 2011; **41**:1480–90.
35 Shimizu J, Yamazaki S, Takahashi T, Ishida Y, Sakaguchi S. Stimulation of CD25(+)CD4(+) regulatory T cells through GITR breaks immunological self-tolerance. Nat Immunol 2002; **3**:135–42.
36 Zabransky DJ, Nirschl CJ, Durham NM *et al.* Phenotypic and functional properties of Helios+ regulatory T cells. PLOS ONE 2012; **7**:e34547.
37 Sakaguchi S, Vignali DA, Rudensky AY, Niec RE, Waldmann H. The plasticity and stability of regulatory T cells. Nat Rev Immunol 2013; **13**:461–7.
38 Itoh K, Hirohata S. The role of IL-10 in human B cell activation, proliferation, and differentiation. J Immunol 1995; **154**: 4341–50.
39 Choe J, Choi YS. IL-10 interrupts memory B cell expansion in the germinal center by inducing differentiation into plasma cells. Eur J Immunol 1998; **28**:508–15.
40 Ng TH, Britton GJ, Hill EV, Verhagen J, Burton BR, Wraith DC. Regulation of adaptive immunity; the role of interleukin-10. Front Immunol 2013; **4**:129.
41 Pesenacker AM, Broady R, Levings MK. Control of tissue-localized immune responses by human regulatory T cells. Eur J Immunol 2015; **45**:333–43.
42 Jutley G, Raza K, Buckley CD. New pathogenic insights into rheumatoid arthritis. Curr Opin Rheumatol 2015; **27**: 249–55.
43 Smith JA. Update on ankylosing spondylitis: current concepts in pathogenesis. Curr Allergy Asthma Rep 2015; **15**:489.
44 Floess S, Freyer J, Siewert C *et al.* Epigenetic control of the foxp3 locus in regulatory T cells. PLoS Biol 2007; **5**:e38.
45 Sather BD, Treuting P, Perdue N *et al.* Altering the distribution of Foxp3(+) regulatory T cells results in tissue-specific inflammatory disease. J Exp Med 2007; **204**:1335–47.
46 Ishida T, Ishii T, Inagaki A *et al.* Specific recruitment of CC chemokine receptor 4-positive regulatory T cells in Hodgkin lymphoma fosters immune privilege. Cancer Res 2006; **66**:5716–22.
47 Mercer F, Kozhaya L, Unutmaz D. Expression and function of TNF and IL-1 receptors on human regulatory T cells. PLOS ONE 2010; **5**:e8639.
48 Brinster C, Shevach EM. Costimulatory effects of IL-1 on the expansion/differentiation of CD4+CD25+Foxp3+ and CD4+CD25+Foxp3- T cells. J Leukoc Biol 2008; **84**:480–7.
49 Christenson K, Bjorkman L, Karlsson A, Bylund J. Regulation of neutrophil apoptosis differs after *in vivo* transmigration to skin chambers and synovial fluid: a role for inflammasome-dependent interleukin-1beta release. J Innate Immun 2013; **5**: 377–88.

Supporting information

Additional Supporting information may be found in the online version of this article at the publisher's Web site:

Fig. S1. Synovial Helios$^+$ and Helios$^-$ forkhead box protein 3 (FoxP3)$^+$ T cells show the highest degree of CCR4 expression. The dot-plots show representative stainings of CXCR3, CCR6, CCR4 and CCR7 expression on CD4 T cells plotted against FoxP3 in paired synovial fluid (SF) (a) and peripheral blood (PB) (b) samples. The summary graphs display the frequency of CXCR3-, CCR6-, CCR4- and CCR7-positive Helios$^{+/-}$FoxP3$^+$ T cells as well as Helios$^{+/-}$FoxP3$^-$ T cells in paired synovial fluid (SF) (a) and peripheral blood (PB) (b) samples [$n = 9$ diagnosis: ankylosing spondylitis (SpA)]. The data were compared using the Kruskal–Wallis test together with Dunn's multiple comparison post-test, significance: $^{***}P < 0{\cdot}001$, $^{**}P < 0{\cdot}005$ and $^{*}P < 0{\cdot}05$.

Fig. S2. Co-expression of interleukin (IL)-1R1 and CCR7 enriches for Helios$^-$forkhead box protein 3 (FoxP3)$^+$ cells in peripheral blood (PB) but not in synovial fluid (SF). The summary graphs show the frequencies of

Helios^{-}FoxP3^{+} in PB (a) and SF (b) and the frequencies of Helios^{+}FoxP3^{+} T cells in PB (c) and SF (d) within CD4^{+}CD25^{++} cells or in the different CCR7/IL-1R1 cell subpopulations within the CD4^{+}CD25^{++} cells. Representative fluorescence activated cell sorter (FACS) plots of paired cell samples of PB (e) and SF (f) show the application of the CCR7/IL-1R1 marker combination in distinguishing Helios subsets within CD4^{+}CD25^{+} cells [$n = 4$, diagnosis ankylosing spondylitis (SpA)]. The summary graphs (g,h) depict the frequencies of Helios^{-}FoxP3^{+} cells gained when gating on CD25^{++}IL-1R1^{+} cells compared to using a CD25^{++} gate alone, in PB (g) and SF (h) [$n = 13$, eight SpA and five rheumatoid arthritis (RA)]. For data analysis, the Kruskal–Wallis test together with Dunn's multiple comparison post-test was used when comparing several groups and grouped data were compared using the Wilcoxon's signed-rank test, $^{**}P < 0{\cdot}001$ and $^{***}P < 0{\cdot}0001$.

Fig. S3. Interleukin (IL)-1R1 displays similar expression patterns in peripheral blood (PB) and synovial fluid (SF) joints of both rheumatoid arthritis (RA) and ankylosing spondylitis (SpA). The graphs summarize flow cytometric analysis of the frequencies of IL-R1^{+}forkhead box protein 3 (FoxP3)$^{+}$ cells in paired PB and SF divided into patients diagnosed with SpA and RA (a). Frequencies of IL-1R1 expressing Helios^{+} and Helios^{-}FoxP3^{+} cells of each subpopulation is shown for SpA (b) and RA (c) and the frequencies of CD25^{++} cells in the IL-1R1^{+}FoxP3^{+} cell population in PB and SF from patients diagnosed with SpA and RA, respectively (d) [$n = 14$, nine SpA and five RA]. Data were compared using Wilcoxon's signed-rank test, $^{**}P < 0{\cdot}001$ and $^{***}P < 0{\cdot}0001$.

